Tree Physiology 00, 1–12
https://doi.org/10.1093/treephys/tpad107

Research paper

Hydraulic traits and photosynthesis are coordinated with trunk sapwood capacitance in tropical tree species

Yang Wei[1,2], Ya-Jun Chen[3,4], Zafar Siddiq[5], Jiao-Lin Zhang[3], Shu-Bin Zhang[3], Steven Jansen[6] and Kun-Fang Cao[1,2,7]

[1]State Key Laboratory for Conservation and Utilization of Subtropical Agro-Bioresources, College of Forestry, Guangxi University, NO. 100 Daxuedonglu, Nanning 530004, Guangxi, China; [2]Guangxi Key Laboratory of Forest Ecology and Conservation, College of Forestry, Guangxi University, NO. 100 Daxuedonglu, Nanning 530004, Guangxi, China; [3]CAS Key Laboratory of Tropical Forest Ecology, Xishuangbanna Tropical Botanical Garden, Chinese Academy of Sciences, Menglun, Mengla 666303, Yunnan, China; [4]Yuanjiang Savanna Ecosystem Research Station, Xishuangbanna Tropical Botanical Garden, Chinese Academy of Sciences, Yuanjiang 653300, Yunnan, China; [5]Department of Botany, Government College University, Katchery Road, Lahore 54000, Punjab, Pakistan; [6]Institute of Botany, Ulm University, Albert-Einstein-Allee 11, Ulm 89081, Baden-Wurttemberg, Germany; [7]Corresponding author (kunfangcao@gxu.edu.cn)

Received March 12, 2023; accepted August 28, 2023; Handling Editor Frederick Meinzer

Water stored in trunk sapwood is vital for the canopy to maintain its physiological function under high transpiration demands. Little is known regarding the anatomical properties that contribute to the hydraulic capacitance of tree trunks and whether trunk capacitance is correlated with the hydraulic and gas exchange traits of canopy branches. We examined sapwood capacitance, xylem anatomical characteristics of tree trunks, embolism resistance, the minimal xylem water potential of canopy branches, leaf photosynthesis and stomatal conductance in 22 species from a tropical seasonal rainforest and savanna. The results showed that the mean trunk sapwood capacitance did not differ between the two biomes. Capacitance was closely related to the fiber lumen fraction and fiber wall reinforcement and not to the axial and ray parenchyma fractions. Additionally, it was positively correlated with the theoretical hydraulic conductivity of a trunk and the specific hydraulic conductivity of branches, and showed a trade-off with branch embolism resistance. Species with a high trunk sapwood capacitance maintained less negative canopy water potentials in the dry season, but higher leaf photosynthetic rates and stomatal conductance in the wet season. This study provides a functional link among trunk sapwood capacitance, xylem anatomy, canopy hydraulics and photosynthesis in tropical trees.

Keywords: embolism resistance, fiber lumen, fiber wall reinforcement, hydraulic safety, photosynthetic rate.

Introduction

According to the tension-cohesion theory, canopy transpiration induces negative pressure that drives xylem water transport from the roots through the stems to the canopy in woody plants. However, under conditions of high transpiration or soil water deficit, low xylem water potentials may increase the level of xylem embolism and thus cause hydraulic dysfunction (Tyree and Sperry 1989, Ozanne et al. 2003, Larter et al. 2015, Nakamura et al. 2017). Previous studies have shown that water in the trunk can compensate, at least to a certain extent, for water depletion in the canopy induced by transpiration (Goldstein et al. 1998, Gartner and Meinzer 2005, Hao et al. 2013, Chen et al. 2016). The amount of water released from trunk storage tissues can contribute between 10 and 50% of the total daily transpiration in trees, depending on the tree architecture and habitat (Holbrook and Sinclair 1992, Goldstein et al. 1998, Phillips et al. 2003, Steppe and Lemeur 2004, Scholz et al. 2007, Kobayashi and Tanaka 2010).

Sapwood capacitance, defined as the ratio of the change in cumulative water release per wood volume to the change in water potential, is typically used to quantify the ability of sapwood to store water (Meinzer et al. 2003). The released water is stored in the lumina and cell walls of dead cell types (vessels, tracheids or fibers) and in living cells, such as

the parenchyma and living fibers (Berry and Roderick 2005, Pfautsch et al. 2015, Chen et al. 2016, Jupa et al. 2016). Capacitance can be measured in different organs, such as the trunk wood, root xylem and shoots (Scholz et al. 2011, Jiang et al. 2021, Bucci et al. 2023). The water release process can be separated into three phases: an initial phase with rapid water release (Phase I), a second phase with slow water release (Phase II) and a third phase (Phase III) due to embolism formation (Tyree and Yang 1990, Hunt et al. 1991). Water released in Phase I is mainly withdrawn from the capillary spaces and lumina of vessels, tracheids or fibers. By contrast, the water released in Phase II is discharged from living cells, such as the axial or ray parenchyma, and this process usually occurs at more negative water potentials (Tyree and Yang 1990, Tyree and Zimmermann 2002). The magnitude of capacitance in different phases has been reported to be strongly related to the anatomical characteristics of the xylem tissues (Scholz et al. 2007, Jupa et al. 2016). For example, a recent study showed that Phase I sapwood capacitance in branches and roots strongly correlates with the fiber/tracheid lumen area in temperate tree species (Jupa et al. 2016). Therefore, fiber lumen area may contribute to sapwood capacitance, which has been linked to wood density (WD) (Ziemińska et al. 2013). Additionally, the xylem parenchyma tissue plays multiple roles in plants, including water storage (tissue capacitance) and participation in water delivery between the xylem and phloem (Borchert and Pockman 2005, Morris et al. 2016). In temperate forests, living parenchyma with thinner cell walls contributes more to water release during Phase II (Jupa et al. 2016). However, there is no published evidence on the influence of the fraction of parenchyma cells on the capacitance of the trunk sapwood.

The embolism resistance and hydraulic conductivity of branch xylem are coordinated with its sapwood capacitance (McCulloh et al. 2014, Santiago et al. 2018, Jiang et al. 2021). Embolism resistance is a crucial hydraulic trait that reflects plant adaptations to drought stress, particularly in a tropical seasonal rainforest (TSF) or a savanna (Zhang et al. 2019, Chen et al. 2021). Although previous studies have suggested a trade-off between xylem embolism resistance and sapwood capacitance in branches (Pratt et al. 2007), only a few studies support a link between the trunk sapwood capacitance and embolism resistance in canopy branches (Oliva Carrasco et al. 2014). Both sapwood capacitance and embolism resistance are associated with WD, which is an integrated indicator of the spatial allocation of various cell types (Scholz et al. 2007, Chave et al. 2009, Oliva Carrasco et al. 2014, Jupa et al. 2016). Higher WDs often result in higher resistance to xylem embolism (more negative P_{50} or P_{88}, the xylem water potential at 50 and 88% loss of hydraulic conductivity) and lower sapwood capacitance (Kraft et al. 2010, Liang et al. 2021). In addition, the sapwood capacitance of branches was coordinated with specific hydraulic conductivity, which may be because a high branch capacitance maintains a high water potential in the canopy during branch development, and allows the development of large vessels, thus the high conductivity of branches (Cruiziat et al. 2002). However, branches with large vessels may have low embolism resistance (Levionnois et al. 2021). In addition, high sapwood capacitance enables plants to diminish the occurrence of xylem embolism and thus maintain relatively high conductivity. However, little attention has been paid to the trunk sapwood capacitance and its influence on the hydraulic conductivity of both the trunk and canopy branches. Moreover, higher trunk sapwood capacitance can maintain higher midday water potentials and carbon assimilation (Siddiq et al. 2019).

In tropical regions, forest canopies are usually exposed to high daily evapotranspiration demands due to strong radiation, high temperatures and high vapor pressure deficit (VPD) levels. Water storage in the trunks has been reported to contribute substantially to daily water use (Meinzer et al. 2003, Čermák et al. 2007). However, little is known about the relationship between trunk sapwood capacitance and wood anatomical properties and between trunk sapwood capacitance and embolism resistance of the canopy branches and photosynthetic physiology. Most trees in a TSF are tall and have a large body size, which can store large amounts of water and temporarily replace water loss. By contrast, mature tropical savanna trees have a lower canopy and smaller tree diameter; however, they tend to be more drought tolerant (Chen et al. 2021). The coordination between trunk sapwood capacitance and canopy hydraulic traits and photosynthesis of tropical trees is still unclear and whether there is any common coordination between these traits across the TSF and savanna. Here, we measured the hydraulic capacitance and wood anatomy of trunk sapwood, xylem vulnerability of canopy branches and photosynthetic capacity across 22 tree species, including 16 species from a TSF, and 6 species from a tropical valley savanna. We aimed to characterize (i) the relationship between trunk sapwood capacitance and the hydraulic traits of canopy stem xylem and leaf photosynthetic physiology and (ii) the extent to which the anatomical properties of trunk sapwood contribute to hydraulic capacitance. We hypothesized that high trunk capacitance provides adequate water supply to the canopy crown and thus allows a high photosynthetic rate; however, it may decrease the xylem embolism resistance. We expected that the trunk sapwood capacitance of Phase I would be mainly contributed by the fractions of dead cells, such as fibers or vessels (Jupa et al. 2016). The fractions of axial and ray parenchyma cells can determine the trunk sapwood capacitance of Phase II since the xylem living cells are commonly regarded as a crucial reservoir of water storage (Morris et al. 2016).

Materials and methods

Study site and plant materials

This study was conducted in a TSF and valley savanna in Yunnan Province, SW China. The TSF site is located in the core area of the National Nature Reserve in Mengla County (21°36′N,

101°35′E, a.s.l. ~780 m). The mean annual precipitation is 1493 mm, with 84% of the precipitation falling between May and October, and the average annual temperature is 21.8 °C (Cao et al. 2006). The savanna site was located at the Yuanjiang Savanna Ecosystem Research Station (23°27′N, 102°10′E, a.s.l. ~481 m) in Yuanjiang County. The mean annual temperature is 24.7 °C, with a maximum air temperature of 43 °C. The mean annual precipitation is 732.8 mm, 80% of which falls between May and October (Zhang et al. 2016). For both sites, the rainy season was from May to October and the dry season is from November to April. The aridity indices (the ratio of mean annual precipitation to annual potential evapotranspiration) of the TSF and savanna sites are 0.96 and 0.33, respectively (Zhang et al. 2021).

Based on the species composition of the sample sites, 16 dominant tree species in the TSF and 6 dominant tree species at the savanna site were selected for this study (Table 1) (Chen et al. 2021, Song et al. 2023). However, certain subcanopy tree species have relatively small tree diameters in mature forests; hence, different tree species in the same biome vary greatly in tree diameter. All replicates of each sample species had similar tree diameters to avoid intraspecific variation. We conducted gas exchange measurements and collected branch samples using an 80-m high canopy crane (boom length of 60 m) at the TSF site. As the mean maximum height of the canopy for most selected species at the savanna site was <9 m, we could access the canopy using a 3-m high ladder. Detailed abbreviations for the measured traits are listed in Table 2.

Water potential measurements

We measured the predawn and midday water potentials of canopy branches at both field sites for canopy branches during the dry season after at least three successive sunny days. Ten sun-exposed, healthy canopy branches from five individuals per species were selected and were tagged the day before measurements. Predawn leaf water potential (Ψ_{pd}) was measured before sun rise (06:00–07:00 h solar time). Midday water potential measurements were taken between 12:30 and 14:30 h. Aluminum foil was used to bag the leaves 2 h before the midday water potential measurements. We selected terminal twigs from the same branches used for the predawn measurements. Midday branch water potentials (Ψ_{md}) were then estimated based on bagged, non-transpiring leaves. Leaf samples were immediately placed in vapor-saturated sealed bags and were stored in an ice box after excision. All water potential measurements were conducted with a pressure chamber (PMS Instruments 1505D, Albany, OR, USA) within 1 h of sample collection. We defined the midday stem water potential (Ψ_{md}) during the dry season as the seasonal minimal xylem water potential (Ψ_{min}). The difference between predawn and midday water potential ($\Delta\Psi$) was calculated to evaluate the maximal decline of xylem water potential during the day.

Gas exchange measurements

Gas exchange measurements were performed during the wet season of 2021. Five mature, sun-exposed, healthy leaves from five individuals per species were selected for gas exchange measurements using a portable photosynthesis measurement system (LI-COR LI-6400XT, Lincoln, Nebraska, USA) between 09:00 and 11:30 h on a sunny day. The chamber temperature during the measurement was 22 °C, and the VPD was ~0.9 kPa. The air CO_2 concentration in the chamber was maintained at 400 μmol mol^{-1} and the PPFD was maintained at 1200 μmol m^{-2} s^{-1}. The maximum photosynthetic rate (A_{max}, μmol m^{-2} s^{-1}) and the maximum stomatal conductance (g_s, mol m^{-2} s^{-1}) were recorded in the steady state.

Xylem vulnerability curves

We first estimated the maximal vessel length (MVL) of each species using an air-injection technique (Gao et al. 2019). Branches ($n = 5$) 1.5 m long were cut and injected with air from the distal ends, with the basal end immersed in water. Then, we cut the branch from the basal end at a 1-cm interval until a continuous stream of tiny bubbles was observed. The remaining branch length plus 1 cm was defined as the MVL of the branch.

The xylem vulnerability curves (VCs) of the canopy branches were determined using a bench dehydration method during the wet season of 2022 (Sperry et al. 1988, Torres-Ruiz et al. 2015). Approximately 20 branches (1.5 × the length of MVL) from four to six individuals per tree species were sampled during the early morning and were instantly transported to the laboratory. Three to five leaves on two twigs were covered with aluminum foil to avoid water loss and were then dehydrated in a dry environment in a laboratory for a given time to cover a wide range of water potentials. Next, the branches were equilibrated in black plastic bags with wet paper towels for at least 1 h. The xylem water potential (Ψ) was determined by taking the average of the two selected twigs. Subsequently, the branches were submerged in water, and the lateral branches were cut under water to relax the xylem tension for ~2 h (Wheeler et al. 2013). The segment was then attached to a hydraulic conductivity apparatus, and a digital liquid flow meter (Bronkhorst Liqui-Flow L13, Veenendaal, Netherlands) was used to record the flow rate. The pressure gradient was driven by the gravity of a 30-cm water column. The segments were then flushed with a degassed 20 mM KCl solution at a pressure of 0.15 MPa to remove air bubbles for 30–60 min until no bubbles were observed at the distal ends. The hydraulic conductance (K, kg m s^{-1} MPa^{-1}) was measured before and after flushing. The percentage loss of conductivity (PLC) was calculated as follows:

$$K_i = \frac{J_V}{(\Delta P/\Delta L)}, \quad (1)$$

$$PLC = 100 \times \frac{(K_{max} - K_i)}{K_{max}}, \quad (2)$$

Table 1. List of the 22 tree species studied in a TSF and savanna site.

Species	Family	Code	DBH (cm)	Height (m)
Seasonal rainforest species				
Ailanthus fordii	Simaroubaceae	AF	30.4–39.4	20–25
Barringtonia fusicarpa	Lecythidaceae	BF	22.5–37.4	19–23
Castanopsis indica	Fagaceae	CI	28.5–37.6	23–28
Colona thorelii	Malvaceae	CT	34–51.5	29–32
Drypetes hoaensis	Putranjivaceae	DH	25.5–35	23–31
Garcinia cowa	Clusiaceae	GC	29–36	19–25
Garuga floribunda var. *gamblei*	Burseraceae	GG	32.5–54	26–38
Gironniera subaequalis	Cannabaceae	GS	32–43.6	26–33
Litsea dilleniifolia	Lauraceae	LD	17.5–23	32–35
Parashorea chinensis	Dipterocarpaceae	PC	35–37	24–27
Pterospermum menglunense	Malvaceae	PM	24–31.2	24–28
Pometia pinnata	Sapindaceae	PP	33–37.4	23–27
Pseuduvaria trimera	Annonaceae	PT	29–32	24–25
Semecarpus reticulatus	Anacardiaceae	SR	34–67	27–39
Sloanea tomentosa	Elaeocarpaceae	ST	41–48	34–38
Walsura pinnata	Meliaceae	WP	29–32	18–22
Savanna species				
Garuga pinnata[1]	Burseraceae	GP	20–40	7–8
Haldina cordifolia[1]	Rubiaceae	HC	19.2–28.5	8–9
Lannea coromandelica[1]	Anacardiaceae	LC	25–29	8–9
Olea ferruginea	Oleaceae	OF	8.0–9.4	4–5
Polyalthia cerasoides[1]	Annonaceae	POC	11–12	8–9
Terminalia franchetii[1]	Combretaceae	TF	10–14	7–8

DBH, diameter at breast height.
[1]Denotes deciduous species; the remaining species are all evergreen.

where J_V was the flow rate (kg s^{-1}) and $\Delta P/\Delta L$ was the pressure gradient per stem segment length (MPa m^{-1}); and K_i and K_{max} were the hydraulic conductivity before and after flushing. The sapwood-specific conductivity (K_s, kg m^{-1} s^{-1} MPa^{-1}) was calculated by dividing K_{max} with the sapwood area (m^2), which was measured in the middle of the segment.

Trunk sapwood capacitance

Sapwood capacitance was measured by constructing water release curves using trunk sapwood samples (Meinzer et al. 2003, Siddiq et al. 2019). All samples were collected early in the morning in April 2021 to ensure that well-hydrated cores were obtained. We drilled cores of 1.5 cm length from the outer sapwood of the rainforest trees (TSF) or of 0.5 cm length from the savanna trees (four individuals per species) at 1.3 m above the soil surface using a 5-mm increment borer. Tree cores were sealed in 15-mL plastic tubes, transported to the laboratory and rehydrated in distilled water for at least 4 h. First, we determined the volume of fresh wood (V, cm^3) using the water displacement method. Then, the cores were cut into 5-mm segments and were used to cover the bottom of a sample cup for water potential measurements using a Dew Point Potential Meter (Decagon Devices WP-4C, Pullman, Washington, USA). The equipment was warmed for 30 min before placing the segments into the chamber, which was run continuously. After measuring the water potential (Ψ_x, MPa), the sample cup was removed from the WP-4C device and was weighed using an analytical balance (0.0001 g) to obtain a constant fresh mass (W_f, g). Following this, the sample was dried at room temperature to reach a wide range of dehydration stages during which the water potential and fresh weight were periodically determined at 20-min and 6-h intervals, depending on the dehydration rate. This approach was applied until the water potential reached ~−8 MPa. Finally, the sample dry mass (W_d, g) was determined after oven-drying at 70 °C for >72 h. The WD (g cm^{-3}) was calculated as: $WD = W_d/V$.

A water release curve was constructed as the cumulative sapwood water release (CWR, kg m^{-3}) against Ψ_x, where the CWR was calculated as:

$$CWR = (1 - RWC) \times (W_s - W_d) \times \frac{1000 \times WD}{W_d}, \quad (3)$$

where W_s is sapwood saturated weight after rehydration, and RWC is the relative water content at each drying stage, calculated as:

$$RWC = \frac{(W_f - W_d)}{(W_s - W_d)}. \quad (4)$$

Table 2. Abbreviations and units of the traits examined in the study.

Variables	Abbreviations	Unit
Sapwood anatomical traits		
Trunk sapwood density	WD	g cm^{-3}
Trunk sapwood SWC	SWC	g g^{-1}
Hydraulic weighted diameter	D_h	μm
Fiber wall reinforcement	FWR	$(\mu m\ \mu m^{-1})^2$
Vessel fraction	VF	%
Axial parenchyma fraction	APF	%
Ray parenchyma fraction	RPF	%
Fiber wall fraction	FWF	%
Fiber lumen fraction	FLF	%
Tracheid fraction	TF	%
Hydraulic and photosynthetic traits		
Branch sapwood specific hydraulic conductivity	K_S	kg m^{-1} s^{-1} MPa^{-1}
Trunk sapwood theoretical hydraulic conductivity	K_{th}	kg m^{-1} s^{-1} MPa^{-1}
Xylem water potential at 50% loss of hydraulic conductivity	P_{50}	MPa
Xylem water potential at 88% loss of hydraulic conductivity	P_{88}	MPa
Predawn leaf water potential	Ψ_{pd}	MPa
Minimum branch water potential	Ψ_{min}	MPa
Difference between predawn and midday branch water potential	$\Delta\Psi$	MPa
Leaf maximum photosynthetic rate	A_{max}	μmol m^{-2} s^{-1}
Leaf maximum stomatal conductance	g_s	mol m^{-2} s^{-1}
Water storage capacity		
Sapwood capacitance during Phase I	C_I	kg m^{-3} MPa^{-1}
Sapwood capacitance during Phase II	C_{II}	kg m^{-3} MPa^{-1}
Sapwood capacitance during the day	$C_{pd\text{-}md}$	kg m^{-3} MPa^{-1}
Sapwood water potential at the turgor loss point	$\Psi_{tlp\text{-}x}$	MPa

A total of 15–20 Ψ_x–CWR paired values were used to construct a water release curve for each species. Water release curves were analyzed using the hyperbolic model $y = ax/(b + x)$ (Jupa et al. 2016). The sapwood capacitances C_I (capacitance of the initial linear portion, from Ψ = 0 to b MPa) and C_{II} (capacitance of the second nearly linear portion, from Ψ = b to −8 MPa) were determined by two different nearly linear phases of a water release curve (Meinzer et al. 2003).

The sapwood water potential at the turgor loss point ($\Psi_{tlp\text{-}x}$) was calculated using a spreadsheet application (https://sites.lifesci.ucla.edu/eeb-sacklab/protocols/) (Santiago et al. 2018, De Guzman et al. 2021). The sapwood capacitance over the Ψ range during the day ($C_{pd\text{-}md}$) was defined as

$$C_{pd\text{-}md} = \frac{(CWR_{md} - CWR_{pd})}{(\Psi_{pd} - \Psi_{md})}, \quad (5)$$

where CWR_{md} is the midday CWR and CWR_{pd} is the predawn CWR; $C_{pd\text{-}md}$ was used to evaluate the water release ability between predawn and midday, as $\Psi_{tlp\text{-}x}$ was less negative than Ψ_{md} for most tree species in this study (Zhang et al. 2013, Ziemińska et al. 2020).

Trunk sapwood anatomy

The cores used for sapwood capacitance measurements were preserved in 15-mL plastic tubes with FAA solutions for at least 3 months to soften the samples. A 5-mm long core sample from the outer sapwood was sectioned into 10-μm thick slices with a sliding microtome (Leica SM2010R, Nusslock, Germany), and the slices were stained with Safranin and Alcian blue solutions. Approximately 30 images were captured at 40× magnification using a Leica microscope (Leica DM3000 LED, Wetzlar, Germany). Tissue fractions or cell dimensions were identified and were drawn manually using the polygon selection tool in ImageJ software (Fiji, National Institutes of Health, USA) (Schindelin et al. 2012). According to the Hagen-Poiseuille law, the theoretical hydraulic conductivity of trunk sapwood (K_{th}, kg m^{-1} s^{-1} MPa^{-1}) was calculated as (Tyree and Zimmermann 2002, Poorter et al. 2010):

$$K_{th} = \frac{\pi \rho D_h^4}{128\eta} \times VD, \quad (6)$$

where π is the circular constant of 3.14, ρ is the density of water (997.05 kg m^{-3} at 25 °C), VD is the vessel density and η is the viscosity of water (0.8937 × 10^{-9} MPa s at 25 °C). The hydraulically weighted vessel diameter (D_h; μm) was calculated as (Sterck et al. 2008):

$$D_h = \left[\left(\frac{1}{n}\right)\sum_{i=1}^{n} D_i^4\right]^{\frac{1}{4}}. \quad (7)$$

Statistical analysis

All statistical analyses were performed using R software (version 4.2.0, R Core Team), and the relationships between key traits were examined using Pearson's correlation (Figure S1); data were log-transformed to meet normality and homoscedasticity if necessary. Water release curves were analyzed using the nls function (Figure S2). The trunk capacitance and WD of 14 tree species from a tropical rainforest and 10 tree species from a subtropical forest were collected from the literature, and the data from this study were used to determine whether there was a common relationship between these two sites. Xylem VCs were fitted with a Weibull model using the fitplc package. A total of 20–30 PLC values for each species were used to construct VCs (Ogle et al. 2009, Duursma and Choat 2017). Based on the fitted curves, we generated values of P_{50} and P_{88}, the xylem water potential at 50 and 88% loss of hydraulic conductivity. A few of the hydraulic traits of the savanna trees were retrieved from Chen et al. (2021). Given that evolutionary history may have affected our analyses, a phylogenetic tree of the 22 tree species from the TSF and savanna sites was constructed using the phylo.maker function of the V.PhyloMaker package and the ggtree package (Figure S3 available as Supplementary data at *Tree Physiology* Online). The phylogenetic signals of the 17 functional traits were analyzed using the phylosig function of the phytools package to verify the influence of phylogenetic relationships on the functional traits (Blomberg et al. 2003). By combining the phylogenetic tree with the phylogenetic signals, the phylogenetic *K*-values ranged from 0.172 to 0.862. Phylogenetic *P*-values were >0.05, indicating that the functional traits were not affected by the evolutionary history of the tree species studied (Table S1 available as Supplementary data at *Tree Physiology* Online). To analyze the association of multiple traits and species grouping in the multivariate space of traits, a principal component analysis (PCA) of 17 traits from the 22 tree species from the two sites was conducted using the FactoMineR package (Lê et al. 2008).

Results

The association between trunk sapwood capacitance and branch traits

Trunk sapwood capacitance was associated with embolism resistance in canopy branches and a positive correlation between C_l and either P_{50} or P_{88} was observed (R^2 = 0.30, $P < 0.01$; $R^2 = 0.47$, $P < 0.001$, respectively) (Figure 1a and c). Moreover, WD was negatively correlated with P_{50} (R^2 = 0.31, $P < 0.01$) (Figure S4a available as Supplementary data at *Tree Physiology* Online). Trunk sapwood capacitance is associated with the xylem hydraulic efficiency of the trunk or canopy branches. The K_{th} was positively correlated with C_l (R^2 = 0.30, $P < 0.01$) (Figure 1d), and the correlation between K_s and C_l was significantly positive when *Garuga pinnata* was excluded (R^2 = 0.32, $P < 0.01$) (Figure 1b).

The coordination between trunk sapwood capacitance and canopy physiology

Trunk sapwood capacitance during the day ($C_{pd\text{-}md}$) was closely associated with the daily canopy water status. An exponential relationship was found between $C_{pd\text{-}md}$ and the seasonal minimum branch water potential (Ψ_{min}) across the tree species studied (R^2 = 0.93, $P < 0.001$) (Figure 2a) despite a linear correlation between Ψ_{min} and $C_{pd\text{-}md}$ in the TSF (R^2 = 0.53, P = 0.001) and savanna (R^2 = 0.76, P = 0.024). Additionally, $C_{pd\text{-}md}$ was negatively associated with the difference between predawn and midday branch water potential ($\Delta\Psi$) across the species studied (R^2 = 0.59, $P < 0.001$) (Figure 2c). Accordingly, tree species with a high trunk capacitance showed a smaller proportional decline in daily water potential. The WD was negatively related to Ψ_{min} (R^2 = 0.30, $P < 0.01$) (Figure S4b available as Supplementary data at *Tree Physiology* Online), and furthermore, C_l was positively correlated with A_{max} (R^2 = 0.21, $P < 0.001$) and g_s (R^2 = 0.26, $P < 0.001$) (Figure 2b and d).

The association between the 17 traits of the 22 tree species from the TSF and the savanna was evaluated using PCA (Figure 3a). The first axis of the PCA explained 47.5% of the variation in the traits. The positive loadings were associated with traits of water storage capacity (C_l, C_{ll}, SWC and FLF), while negative loadings, such as WD and FWR, were associated with structural resistance. The second axis accounted for 14.3% of the trait variation and was associated with hydraulic conductivity (i.e., VF, APF and K_{th}). The tree species from the TSF and a savanna were well separated along the second axis (Figure 3b.

Trunk sapwood capacitance and its structural determinants

Trunk sapwood capacitance varied greatly among species in TSFs and savanna sites. At the TSF site, the C_l ranged from 139.32 kg m^{-3} MPa^{-1} in *Walsura pinnata* to 508.08 kg m^{-3} MPa^{-1} in *Colona thorelii*. At the savanna site, C_l varied from 166.65 kg m^{-3} MPa^{-1} in *Olea ferruginea* to 434.76 kg m^{-3} MPa^{-1} in *Lannea coromandelica* (Table S2 available as Supplementary data at *Tree Physiology* Online). Although five of the six tree species at the savanna site were deciduous, the magnitude of capacitance showed no difference between the evergreen and deciduous tree species among the 22 species studied (P = 0.75). The magnitude of C_l was ~10–66 times the value of C_{ll} for TSF and savanna trees, respectively. After calculation with predawn and midday water potential, $C_{pd\text{-}md}$ was significantly decreased compared with C_l and ranged from 2.78 kg m^{-3} MPa^{-1} in *O. ferruginea* to 165.81 kg m^{-3} MPa^{-1} in *Gironniera subaequalis.* Our results showed that both trunk C_l and C_{ll} were negatively related to sapwood density (WD) (Figure S1 available as Supplementary data at *Tree Physiology* Online and Figure 4b). The data from

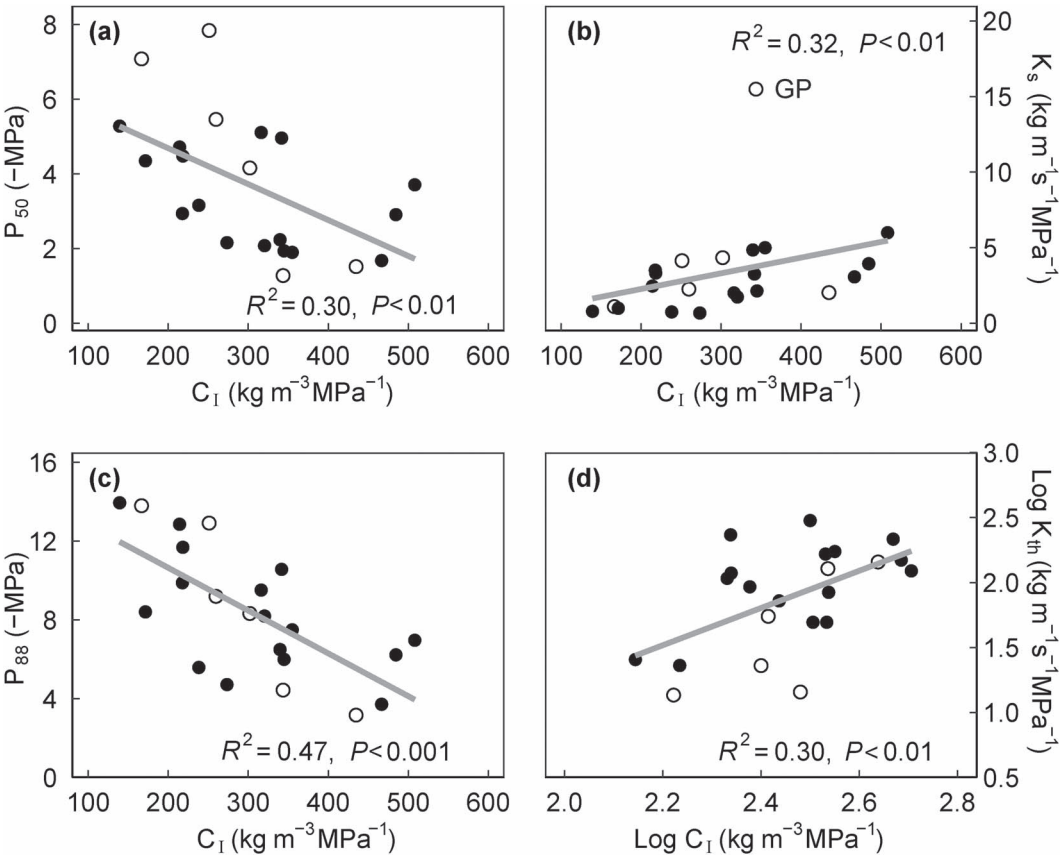

Figure 1. Relationships between trunk sapwood capacitance and branch hydraulic traits (a–d) across 22 tree species from the TSF (black circles, $N = 16$) and savanna (white circles, $N = 6$). Each symbol represents a mean value based on four individuals. The outlier (*Garuga pinnata*; GP) in (b) is excluded from the linear regression analysis. P_{50}, xylem water potential at 50% loss of hydraulic conductivity; P_{88}, xylem water potential at 88% loss of hydraulic conductivity; K_s, branch sapwood specific hydraulic conductivity; K_{th}, trunk sapwood theoretical hydraulic conductivity.

this study, together with an additional 24 tropical and subtropical tree species from the literature, exhibited an exponential decay relationship between WD and trunk capacitance ($R^2 = 0.82$, $P < 0.001$) (Figure 4a). Additionally, a close correlation exists between saturated water content (SWC) and C_I ($R^2 = 0.82$, $P < 0.001$) (Figure 4c). The sapwood water potential at the turgor loss point ($\Psi_{tlp\text{-}x}$) showed a positive relationship with C_I (Figure 4d) and a negative relationship with WD (Figure S4c available as Supplementary data at *Tree Physiology* Online). Moreover, C_I had a negative correlation with fiber wall reinforcement ($R^2 = 0.68$, $P < 0.001$) (Figure 4e) and a strongly positive correlation with fiber lumen fraction (FLF) ($R^2 = 0.56$, $P < 0.001$) (Figure 4f). At the same time, there was no significant correlation between C_I and vessel fractions (Figure S3S1 available as Supplementary data at *Tree Physiology* Online). The C_{II} was independent of the axial and ray parenchyma fractions ($R^2 = 0.11$, $P = 0.14$; $R^2 = 0.002$, $P = 0.84$) (Figure 4g and h).

Significant interspecific differences exist in xylem anatomical characteristics; however, no significant differences were observed between the TSF and savanna trees (Figure S5 available as Supplementary data at *Tree Physiology* Online). For all 22 tree species, the fiber wall fraction had the lowest CV (27.17%), ranging from 9.71% (*Haldina cordifolia*) to 47.44% (*Walsura pinnata*). The CV of the ray parenchyma fraction was 33.35%, ranging from 6.13% (*Castanopsis indica*) to 34.55% in *Barringtonia fusicarpa*. The axial parenchyma fraction had the highest CV (54.89%), ranging from 0.39% (*Sloanea tomentosa*) to 22.91% (*Garcinia cowa*). The CV of the fiber lumen and vessel fractions were 52.06 and 34.47%, respectively. In only two species, *Castanopsis indica* and *Haldina cordifolia*, the vessels were surrounded by tracheid cells, with tracheid fractions of 10.5 and 28.22%, respectively.

Discussion

The results of our study show that the trunk sapwood capacitance of trees from savanna and rainforest sites is largely driven by fiber characteristics, with multifunctional consequences for the embolism resistance and hydraulic conductivity of canopy stems, the xylem water potential of the canopy and leaf gas exchange.

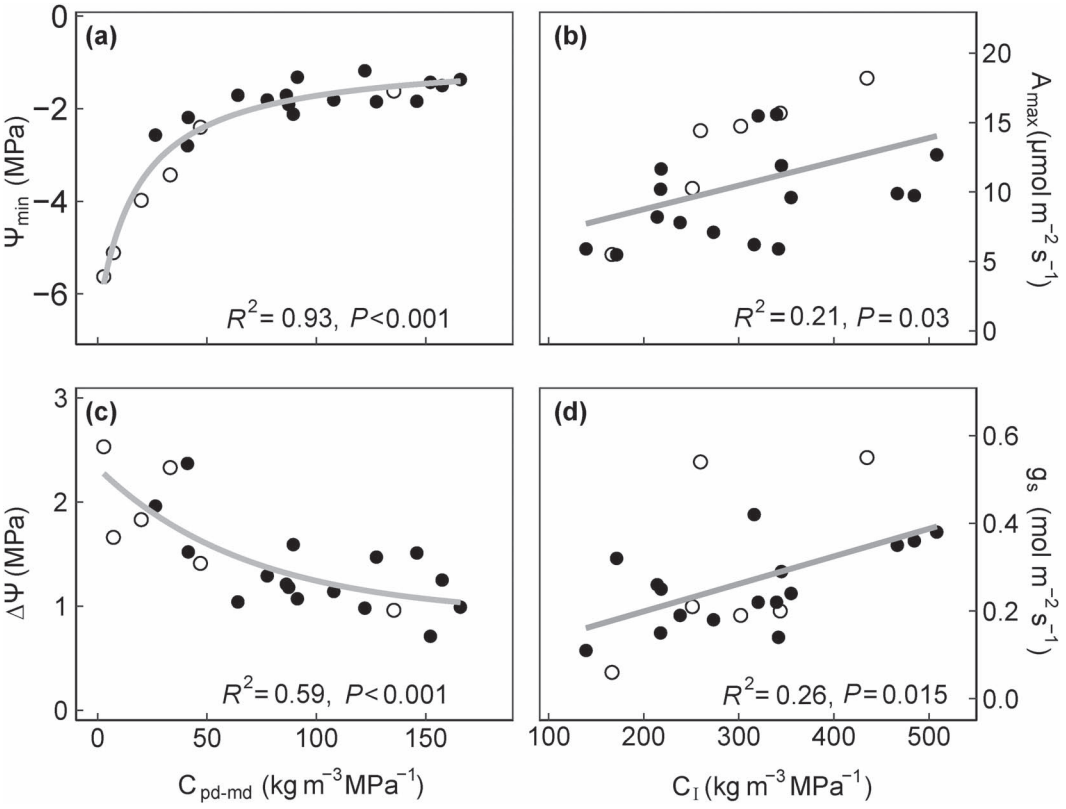

Figure 2. Relationship between trunk sapwood capacitance during the day (C_{pd-md}) and (a) minimum water potential (Ψ_{min}) of stem xylem measured in the dry season, and (c) the difference between predawn and midday branch water potential ($\Delta\Psi$). Relationship between C_l (trunk sapwood capacitance during Phase I) and (b) maximum photosynthetic rate (A_{max}) and (d) maximum stomatal conductance (g_s). Each dot represents a tree species from the TSF (black circles, N = 16) or savanna (white circles, N = 6).

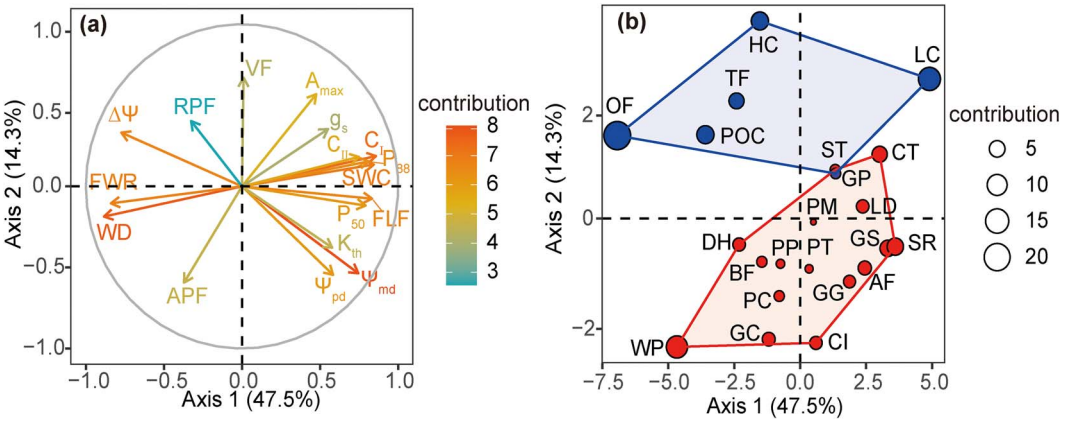

Figure 3. The PCA of 17 traits from 22 tree species. (a) The loadings of 17 traits on the first and second axes; (b) species loading on the first and second axes, red and blue circles represent the TSF (N = 16) and savanna (N = 6), respectively. The color gradient and circle size represent the contributions of traits (a) or species (b) to the first and second axes. Species acronyms and trait abbreviations are provided in Tables 1 and 2, respectively.

High trunk sapwood capacitance was associated with low embolism resistance in canopy stems

Our results revealed that high trunk sapwood capacitance was associated with low embolism resistance in the canopy branches. If high trunk sapwood capacitance can supply a large volume of water to a tree canopy, it may not be necessary for the tree to invest in the high embolism resistance of the xylem in branches. By contrast, species with a relatively low trunk sapwood capacitance could benefit from increased branch embolism resistance (more negative P_{50} and P_{88}) to adapt to low xylem water potentials, which may induce hydraulic dysfunction during severe drought. Accordingly, water storage and embolism resistance are contrasting mechanisms by which plants cope with episodic droughts (Pivovaroff et al. 2015).

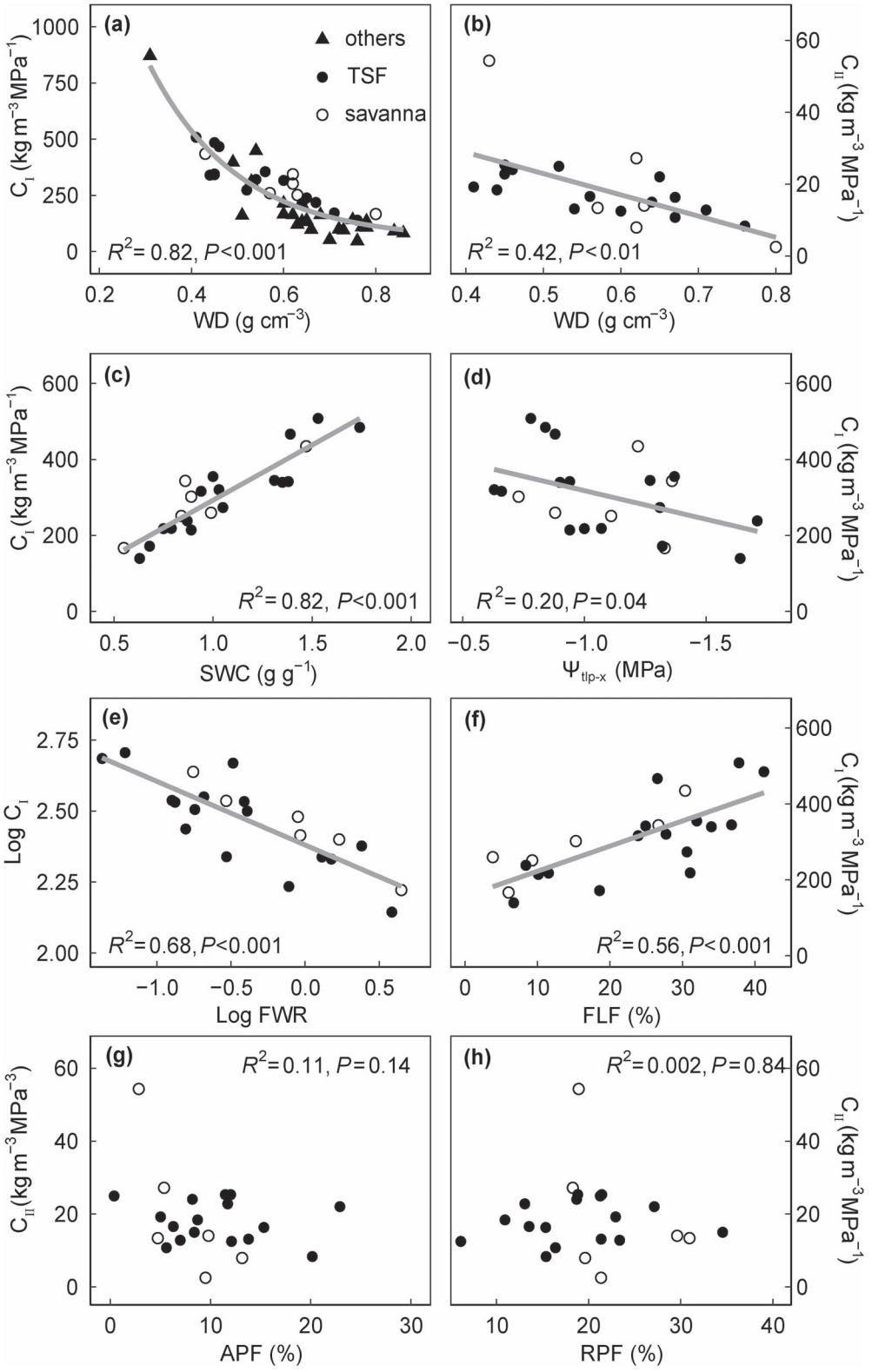

Figure 4. The relationship between mean values (N = 4) of trunk sapwood capacitance during Phases I and II (C_I and C_{II}) of water release and between anatomical parameters in trunk sapwood across 22 tree species from a TSF (black circles, N = 16) and a savanna (white circles, N = 6). (a) Between C_I and sapwood density (WD), the data of tropical and subtropical tree species from Siddiq et al. (2019) and Oliva Carrasco et al. (2014), as indicated by triangles, were collected to establish a robust relationship across 46 tree species (y = 52.28 + 3895.13exp(−5.21x)); (b) between C_{II} and WD; (c) between C_I and SWC; (d) between C_I and turgor loss point of sapwood (Ψ_{tlp-x}); (e) between C_I and fiber wall reinforcement (FWR); (f) between C_I and FLF; (g, h) between C_{II} and the fraction of axial and ray parenchyma (APF and RPF).

Therefore, our results suggest a trade-off between the trunk sapwood capacitance and xylem embolism resistance in the branches. Moreover, the inverse correlation between the trunk sapwood capacitance and branch xylem embolism resistance suggests that tree species with high trunk sapwood capacitance probably enable the development of wide vessels in both the trunk and branch xylem. This may favor the stable maintenance of xylem water transport (K_{th} and K_s) and may come at the expense of reducing xylem embolism resistance.

Our data suggest that there is coordination between transport efficiency and sapwood capacitance. Trunk sapwood capacitance positively correlated with trunk and branch hydraulic conductivity (K_{th} and K_s) in TSF and tropical savanna trees, demonstrating that a high trunk sapwood capacitance could promote xylem water transport efficiency in both the trunk and branches. Time lags between crown and basal sap flow in tropical trees and lianas have proven the important role of trunk water storage (Burgess and Dawson 2007, Chen et al. 2016). Our observations illustrate that trunk sapwood capacitance was functionally achieved by optimizing xylem transport efficiency across tropical tree species in both the trunk and branch xylem.

Trunk sapwood capacitance affects xylem water potential and the leaf gas exchange of the tree canopy

Our findings show that high trunk sapwood capacitance can effectively buffer water stress in tree canopies. In this study, $C_{pd\text{-}md}$ was observed to reflect the water release ability between predawn and midday. Unlike C_l, $C_{pd\text{-}md}$ showed a significant difference between TSF and the tropical savanna tree species ($P = 0.014$). This may result from much lower Ψ_{pd} and Ψ_{md} in the savanna tree species and therefore decreased the values of $\Delta CWR/\Delta\Psi$. Our results indicated that tree species with higher capacitance experienced less negative branch water potential during the dry season. Moreover, savanna tree species were observed to undergo a relatively large change in Ψ_{min} due to their smaller tree size, which limits the storage volume for water. Another explanation for this discrepancy may emerge from higher potential transpiration rates and relatively lower soil water content in the savanna, which is reflected in the lower Ψ_{pd} of the savanna tree species during the dry season. Therefore, our observations revealed that tropical tree species with high trunk capacitance may mobilize large amounts of stored water to buffer the decline in diurnal branch water potential. This is due to canopy transpiration in the morning, thus, a fairly well hydrated canopy is sustained.

Furthermore, sapwood capacitance enhanced A_{max} and g_s as revealed by the positive correlation between C_l and A_{max} and between C_l and g_s. As stated above, trunk capacitance was positively associated with K_s; high water transport capacitance permitted high photosynthetic rates, as reported previously (Brodribb and Feild 2000, Zhang and Cao 2009). Moreover, sufficient water supply from trunk storage buffers fluctuations in the water potential of canopy leaves, thereby buffering fluctuations in photosynthetic rates.

Trunk sapwood capacitance is determined by fiber properties

Fiber lumina may be an important source of water in trunk sapwood. Although the proportion of trunk xylem tissues varied across all of the tropical tree species studied, we observed a strong and positive relationship between the FLF and C_l and a negative relationship between fiber wall reinforcement and C_l, which is in agreement with previous studies (Ziemińska et al. 2013, Jupa et al. 2016, Janssen et al. 2020). A large proportion of wood fibers are gas filled before the occurrence of embolism in xylem conduits, based on X-ray microtomography, which provides visual evidence for the vital role of fiber-stored water in the early stages of drought (Suuronen et al. 2013, Jupa et al. 2016). Fiber tissue is broadly defined here, including labriform fibers, fiber tracheids and even living fibers, excluding tracheids (Sano et al. 2011). How exactly the capacitance is linked to these different fiber types is complicated by the morphological and functional continuity between these fiber types; however, further research is required.

High fiber wall fraction and fiber wall reinforcement were closely related to high WD and low SWC (Figure S1 available as Supplementary data at *Tree Physiology* Online). Although there is a relatively large proportion of axial and ray parenchyma in the trunk sapwood xylem, our data showed that the fractions of axial and ray parenchyma cells were not associated with C_l or C_{ll}. As such, xylem parenchyma cells may not have contributed to sapwood capacitance in our study, although they are widely thought to be important tissues for water storage (Vesala et al. 2003, Morris et al. 2016, Aritsara et al. 2021).

Our results showed that a low WD was beneficial for water storage and hydraulic conductivity (greater K_s), which is consistent with previous studies (Oliva Carrasco et al. 2014, Siddiq et al. 2019). The WD is frequently used as a proxy for sapwood capacitance (C_l and C_{ll}). The combined data from different biomes and growth forms in this study and from the literature support a relationship between WD and C_l. Therefore, we observed that tropical tree species with low capacitance and high WD have a rather negative $\Psi_{tlp\text{-}x}$. Tree species with a lower $\Psi_{tlp\text{-}x}$ could slowly release water in a relatively wide range of xylem water potentials (smaller$\Delta CWR/\Delta\Psi$). At the same time, rapid release in the initial stage was observed in tree species with high $\Psi_{tlp\text{-}x}$. Additionally, tree species with high WD would maintain relatively high turgor of living tissues at a lower xylem water potential, which is beneficial for ensuring that living cells function well during mild drought periods. This divergent pattern could improve our understanding of the initial water release from the tropical tree species with differing WDs.

Conclusions

In summary, our data show a trade-off between the trunk sapwood capacitance and embolism resistance of branch xylem

across tree species in TSF and tropical savanna, with fiber lumina being the primary determinant of water storage in trunk sapwood. Moreover, trunk sapwood capacitance buffered water stress in the tree canopy and was positively correlated with the xylem hydraulic efficiency of both trunk and canopy branches and leaf photosynthesis, reflecting the crucial role of trunk capacitance in determining the drought adaptation and physiological performance of the tropical tree species.

Supplementary data

Supplementary data for this article are available at *Tree Physiology* Online.

Conflict of interest

None declared.

Funding

This work was supported by an international collaboration grant (31861133008) from the National Natural Science Foundation of China and the German Research Foundation (DFG, Deutsche Forschungsgemeinschaft, project number 410768178).

Data availability statement

Data are available in Supplementary data at *Tree Physiology* Online.

References

Aritsara ANA, Razakandraibe VM, Ramananantoandro T, Gleason SM, Cao KF (2021) Increasing axial parenchyma fraction in the Malagasy Magnoliids facilitated the co-optimisation of hydraulic efficiency and safety. New Phytol 229:1467–1480.

Berry SL, Roderick ML (2005) Plant-water relations and the fibre saturation point. New Phytol 168:25–37.

Blomberg SP, Garland T Jr, Ives AR (2003) Testing for phylogenetic signal in comparative data: behavioral traits are more labile. Evolution 57:717–745.

Borchert R, Pockman WT (2005) Water storage capacitance and xylem tension in isolated branches of temperate and tropical trees. Tree Physiol 25:457–466.

Brodribb TJ, Feild TS (2000) Stem hydraulic supply is linked to leaf photosynthetic capacity: evidence from New Caledonian and Tasmanian rainforests. Plant Cell Environ 23:1381–1388.

Bucci SJ, Carbonell-Silletta L, Cavallaro A, Arias NS, Campanello PI, Goldstein G, Scholz FG, Pfautsch S (2023) Bark and sapwood water storage and the atypical pattern of recharge and discharge of water reservoirs indicate low vulnerability to drought in *Araucaria araucana*. Tree Physiol 43:248–261.

Burgess SSO, Dawson TE (2007) Using branch and basal trunk sap flow measurements to estimate whole-plant water capacitance: a caution. Plant Soil 305:5–13.

Cao M, Zou X, Warren M, Zhu H (2006) Tropical forests of Xishuangbanna, China. Biotropica 38:306–309.

Čermák J, Kučera J, Bauerle WL, Phillips N, Hinckley TM (2007) Tree water storage and its diurnal dynamics related to sap flow and changes in stem volume in old-growth Douglas-fir trees. Tree Physiol 27:181–198.

Chave J, Coomes D, Jansen S, Lewis SL, Swenson NG, Zanne AE (2009) Towards a worldwide wood economics spectrum. Ecol Lett 12:351–366.

Chen YJ, Bongers F, Tomlinson K et al. (2016) Time lags between crown and basal sap flows in tropical lianas and co-occurring trees. Tree Physiol 36:736–747.

Chen YJ, Choat B, Sterck F et al. (2021) Hydraulic prediction of drought-induced plant dieback and top-kill depends on leaf habit and growth form. Ecol Lett 24:2350–2363.

Cruiziat P, Cochard H, Améglio T (2002) Hydraulic architecture of trees: main concepts and results. Ann For Sci 59:723–752.

De Guzman ME, Acosta-Rangel A, Winter K, Meinzer FC, Bonal D, Santiago LS (2021) Hydraulic traits of Neotropical canopy liana and tree species across a broad range of wood density: implications for predicting drought mortality with models. Tree Physiol 41:24–34.

Duursma R, Choat B (2017) Fitplc - an R package to fit hydraulic vulnerability curves. J Plant Hydraul 4:e002. https://doi.org/10.20870/jph.2017.e002.

Gao H, Chen YJ, Zhang YJ, Maenpuen P, Lv S, Zhang JL (2019) Vessel-length determination using silicone and air injection: Are there artifacts? Tree Physiol 39:1783–1791.

Gartner BL, Meinzer FC (2005) Structure-function relationships in sapwood water transport and storage. In: Holbrook NM, Zwieniecki MA (eds) Vascular transport in plants. Elsevier, Heidelberg, pp 307–331.

Goldstein G, Andrade JL, Meinzer FC, Holbrook NM, Cavelier J, Jackson P, Celis A (1998) Stem water storage and diurnal patterns of water use in tropical forest canopy trees. Plant Cell Environ 21:397–406.

Hao GY, Wheeler JK, Holbrook NM, Goldstein G (2013) Investigating xylem embolism formation, refilling and water storage in tree trunks using frequency domain reflectometry. J Exp Bot 64:2321–2332.

Holbrook NM, Sinclair TR (1992) Water balance in the arborescent palm, *Sabal palmetto*. II. Transpiration and stem water storage. Plant Cell Environ 15:401–409.

Hunt ER, Running SW, Federer CA (1991) Extrapolating plant water flow resistances and capacitances to regional scales. Agric For Meteorol 54:169–195.

Janssen TAJ, Holtta T, Fleischer K, Naudts K, Dolman H (2020) Wood allocation trade-offs between fiber wall, fiber lumen, and axial parenchyma drive drought resistance in neotropical trees. Plant Cell Environ 43:965–980.

Jiang PP, Meinzer FC, Fu XL, Kou L, Dai XQ, Wang HM (2021) Trade-offs between xylem water and carbohydrate storage among 24 coexisting subtropical understory shrub species spanning a spectrum of isohydry. Tree Physiol 41:403–415.

Jupa R, Plavcova L, Gloser V, Jansen S (2016) Linking xylem water storage with anatomical parameters in five temperate tree species. Tree Physiol 36:756–769.

Kobayashi Y, Tanaka T (2010) Water flow and hydraulic characteristics of Japanese red pine and oak trees. Hydrol Process 15:1731–1750.

Kraft NJ, Metz MR, Condit RS, Chave J (2010) The relationship between wood density and mortality in a global tropical forest data set. New Phytol 188:1124–1136.

Larter M, Brodribb TJ, Pfautsch S, Burlett R, Cochard H, Delzon S (2015) Extreme aridity pushes trees to their physical limits. Plant Physiol 168:804–807.

Lê S, Josse J, Husson F (2008) FactoMineR: a package for multivariate analysis. J Stat Softw 25:1–18.

Levionnois S, Jansen S, Wandji RT et al. (2021) Linking drought-induced xylem embolism resistance to wood anatomical traits in Neotropical trees. New Phytol 229:1453–1466.

Liang XY, Ye Q, Liu H, Brodribb TJ (2021) Wood density predicts mortality threshold for diverse trees. New Phytol 229:3053–3057.

McCulloh KA, Johnson DM, Meinzer FC, Woodruff DR (2014) The dynamic pipeline: hydraulic capacitance and xylem hydraulic safety in four tall conifer species. Plant Cell Environ 37:1171–1183.

Meinzer FC, James SA, Goldstein G, Woodruff D (2003) Whole-tree water transport scales with sapwood capacitance in tropical forest canopy trees. Plant Cell Environ 26:1147–1155.

Morris H, Plavcova L, Cvecko P et al. (2016) A global analysis of parenchyma tissue fractions in secondary xylem of seed plants. New Phytol 209:1553–1565.

Nakamura A, Kitching RL, Cao M et al. (2017) Forests and their canopies: achievements and horizons in canopy science. Trends Ecol Evol 32:438–451.

Ogle K, Barber JJ, Willson C, Thompson B (2009) Hierarchical statistical modeling of xylem vulnerability to cavitation. New Phytol 182:541–554.

Oliva Carrasco L, Bucci SJ, Di Francescantonio D et al. (2014) Water storage dynamics in the main stem of subtropical tree species differing in wood density, growth rate and life history traits. Tree Physiol 35:354–365.

Ozanne CM, Anhuf D, Boulter SL et al. (2003) Biodiversity meets the atmosphere: a global view of forest canopies. Science 301:183–186.

Pfautsch S, Renard J, Tjoelker MG, Salih A (2015) Phloem as capacitor: radial transfer of water into xylem of tree stems occurs via symplastic transport in ray parenchyma. Plant Physiol 167:963–971.

Phillips NG, Ryan MG, Bond BJ, McDowell NG, Hinckley TM, Čermák J (2003) Reliance on stored water increases with tree size in three species in the Pacific northwest. Tree Physiol 23:237–245.

Pivovaroff AL, Pasquini SC, De Guzman ME, Alstad KP, Stemke JS, Santiago LS, Field K (2015) Multiple strategies for drought survival among woody plant species. Functi Ecol 30:517–526.

Poorter L, McDonald I, Alarcon A, Fichtler E, Licona JC, Pena-Claros M, Sterck F, Villegas Z, Sass-Klaassen U (2010) The importance of wood traits and hydraulic conductance for the performance and life history strategies of 42 rainforest tree species. New Phytol 185: 481–492.

Pratt RB, Jacobsen AL, Ewers FW, Davis SD (2007) Relationships among xylem transport, biomechanics and storage in stems and roots of nine Rhamnaceae species of the California chaparral. New Phytol 174:787–798.

Sano Y, Morris H, Shimada H, Ronse De Craene LP, Jansen S (2011) Anatomical features associated with water transport in imperforate tracheary elements of vessel-bearing angiosperms. Ann Bot 107:953–964.

Santiago LS, De Guzman ME, Baraloto C, Vogenberg JE, Brodie M, Herault B, Fortunel C, Bonal D (2018) Coordination and trade-offs among hydraulic safety, efficiency and drought avoidance traits in Amazonian rainforest canopy tree species. New Phytol 218:1015–1024.

Schindelin J, Argandacarreras I, Frise E et al. (2012) Fiji: an open-source platform for biological-image analysis. Nat Methods 9:676–682.

Scholz FG, Bucci SJ, Goldstein G, Meinzer FC, Franco AC, Miralles-Wilhelm F (2007) Biophysical properties and functional significance of stem water storage tissues in neotropical savanna trees. Plant Cell Environ 30:236–248.

Scholz FG, Phillips NG, Bucci SJ, Meinzer FC, Goldstein G (2011). Hydraulic capacitance: biophysics and functional significance of internal water sources in relation to tree size. In: Meinzer FC, Lachenbruch B, Dawson TE (eds) Size- and age-related changes in tree structure and function. Springer, Dordrecht, pp 341–361.

Siddiq Z, Zhang YJ, Zhu SD, Cao KF (2019) Canopy water status and photosynthesis of tropical trees are associated with trunk sapwood hydraulic properties. Plant Physiol Biochem 139:724–730.

Song HQ, Wang YQ, Yan CL, Zeng WH, Chen YJ, Zhang JL, Liu H, Zhang QM, Zhu SD (2023) Can leaf drought tolerance predict species abundance and its changes in tropical-subtropical forests? Tree Physiol 43:1319–1325.

Sperry JS, Donnelly JR, Tyree MT (1988) A method for measuring hydraulic conductivity and embolism in xylem. Plant CellEnviron 11:35–40.

Steppe K, Lemeur R (2004) An experimental system for analysis of the dynamic sap-flow characteristics in young trees: results of a beech tree. Funct Plant Biol 31:83–92.

Sterck FJ, Zweifel R, Sass-Klaassen U, Chowdhury Q (2008) Persisting soil drought reduces leaf specific conductivity in scots pine (*Pinus sylvestris*) and pubescent oak (*Quercus pubescens*). Tree Physiol 28:529–536.

Suuronen JP, Peura M, Fagerstedt K, Serimaa R (2013) Visualizing water-filled versus embolized status of xylem conduits by desktop x-ray microtomography. Plant Methods 9:11–23.

Torres-Ruiz JM, Jansen S, Choat B et al. (2015) Direct X-Ray Microtomography Observation Confirms the Induction of Embolism upon Xylem Cutting under Tension. Plant Physiol 167:40–43.

Tyree MT, Sperry JS (1989) Vulnerability of xylem to cavitation and embolism. Annu Rev Plant Physiol 40:19–36.

Tyree MT, Yang SD (1990) Water-storage capacity of Thuja, Tsuga and Acer stems measured by dehydration isotherms. Planta 182:420–426.

Tyree MT, Zimmermann MH (2002) Xylem structure and the ascent of sap. Q Rev Biol 59:475–476.

Vesala T, Holtta T, Peramaki M, Nikinmaa E (2003) Refilling of a hydraulically isolated embolized xylem vessel: model calculations. Ann Bot 91:419–428.

Wheeler JK, Huggett BA, Tofte AN, Rockwell FE, Holbrook NM (2013) Cutting xylem under tension or supersaturated with gas can generate PLC and the appearance of rapid recovery from embolism. Plant Cell Environ 36:1938–1949.

Zhang JL, Cao KF (2009) Stem hydraulics mediates leaf water status, carbon gain, nutrient use efficiencies and plant growth rates across dipterocarp species. Funct Ecol 23:658–667.

Zhang L, Chen YJ, Ma KP, Bongers F, Sterck FJ (2019) Fully exposed canopy tree and liana branches in a tropical forest differ in mechanical traits but are similar in hydraulic traits. Tree Physiol 39:1713–1724.

Zhang SB, Zhang JL, Cao KF (2016) Divergent hydraulic safety strategies in three co-occurring Anacardiaceae tree species in a Chinese savanna. Front Plant Sci 7:2075–2085.

Zhang YB, Yang D, Zhang KY, Bai XL, Wang YS, Wu HD, Ding LZ, Zhang YJ, Zhang JL (2021) Higher water and nutrient use efficiencies in savanna than in rainforest lianas result in no difference in photosynthesis. Tree Physiol 42:145–159.

Zhang YJ, Meinzer FC, Qi JH, Goldstein G, Cao KF (2013) Midday stomatal conductance is more related to stem rather than leaf water status in subtropical deciduous and evergreen broadleaf trees. Plant Cell Environ 36:149–158.

Ziemińska K, Butler DW, Gleason SM, Wright IJ, Westoby M (2013) Fibre wall and lumen fractions drive wood density variation across 24 Australian angiosperms. AoB Plants 5:1–14.

Ziemińska K, Rosa E, Gleason SM, Holbrook NM (2020) Wood day capacitance is related to water content, wood density, and anatomy across 30 temperate tree species. Plant Cell Environ 43:3048–3067.